Radiocarbon, Vol 00, Nr 00, 2024, p 1–16 DOI:10.1017/RDC.2024.37
Selected Papers from the 24th Radiocarbon and 10th Radiocarbon & Archaeology International Conferences, Zurich, Switzerland, 11–16 Sept. 2022

RADIOCARBON VARIATIONS IN ANNUAL TREE RINGS WITH 11-YEAR SOLAR CYCLES DURING 1800–1950

Pavel P Povinec[1]* • Ivan Kontul'[1] • Ivo Svetlik[2]

[1]Department of Nuclear Physics and Biophysics, Faculty of Mathematics, Physics and Informatics, Comenius University, Bratislava, Slovakia
[2]Institute of Nuclear Physics, Czech Academy of Sciences, Prague, Czech Republic

ABSTRACT. The results of radiocarbon variation studies observed in annual tree rings from the NW Pacific (USA Northwest) (Stuiver and Braziunas 1993) and Europe (England, Brehm et al. 2021; Slovakia, Povinec 1977, 1987) are reviewed with the aim of better understanding the 11-year radiocarbon cycle and possible impacts of solar proton events on ^{14}C levels in the atmosphere and biosphere. The average $\Delta^{14}C$ amplitude in tree rings for the period of 1798–1944 was 1.3 ± 0.3‰, the average periodicity was 11 ± 1 years, and the average time shift between the sunspot numbers and $\Delta^{14}C$ records was 3 ± 1 years. A new solar activity minimum (Gleissberg minimum, 1878–1933) has been identified in the $\Delta^{14}C$ data sets from the NW Pacific and England, showing $\Delta^{14}C$ excess of 7‰, comparable to the Dalton minimum (1797–1823). No significant changes in $\Delta^{14}C$ levels were identified that could be associated with solar proton events during 1800–1950.

KEYWORDS: radiocarbon, solar activity, solar proton events, tree rings, wines.

INTRODUCTION

Radionuclides represent unique tracers of environmental processes, which help to study not only processes of their origin, but also their spread in the atmosphere and in Earth's other reservoirs up to their final storage in isotope archives that record their temporal evolution (in tree rings, glaciers, stalagmites/stalactites, corals, freshwater and marine sediments) (e.g., Lal 1999; Beer et al. 2012; Reimer et al. 2020; Brehm et al. 2021). Except for radionuclides of natural origin (e.g., primordial radionuclides such as ^{232}Th, ^{235}U, ^{238}U, and products in their decay chains), and of anthropogenic origin (e.g., ^{3}H, ^{14}C, ^{90}Sr, ^{129}I, ^{137}Cs, Pu isotopes, etc.), released to the environment mainly after atmospheric nuclear weapons tests (global fallout), nuclear accidents (Chernobyl, Fukushima) or from nuclear reprocessing facilities (e.g., Sellafield in UK and Le Hague in France) (Povinec et al. 2013, 2021), an important group of radionuclides, applied in environmental studies, are cosmogenic radionuclides, produced by interactions of cosmic-ray particles mainly in the Earth atmosphere (e.g., ^{3}H, ^{7}Be, ^{10}Be, ^{14}C, ^{22}Na, ^{26}Al, ^{36}Cl, etc.) (Lal and Peters 1967; Beer et al. 2012; Masarik and Beer 1999, 2009).

The radioactive isotope most frequently used in environmental studies has been radiocarbon (^{14}C) due to its suitable half-life (5700 yr) for studying processes over the last 50,000 years, availability in environmental archives, and existing high-sensitivity detection methods, namely accelerator mass spectrometry (AMS). After its production in the atmosphere as a result of interactions of secondary cosmic-ray particles (mainly neutrons) with nitrogen and oxygen, radiocarbon oxidizes to CO and later to CO_2, which, as a result of exchange processes, enters the biosphere and the ocean. The best ^{14}C archives are therefore materials with annually growing mass records, such as tree rings. Radiocarbon has also been important due to its specific stratosphere-troposphere-biosphere mixing, exchange of carbon dioxide with surface ocean, and finally its sequestration into the deep ocean, which is the main reservoir of radiocarbon (Siegenthaler et al. 1980; Bard et al. 1997; Levin and Hesshaimer 2000).

*Corresponding author. Email: pavel.povinec@uniba.sk

Radiocarbon has therefore become a very useful cosmogenic radionuclide, important for better understanding of exchange processes in the environment.

Environmental studies with radionuclide tracers are built on a foundation of many scientific fields, starting from astrophysics (cosmic rays, their production, and variations in the heliosphere), via nuclear physics (nuclear reactions, cross-sections, simulations of production rates), analysis of samples in suitable archives, and finally carbon cycle modeling (e.g., Lal 1999; Beer et al. 2012; Masarik and Beer 1999, 2009; Levin and Hesshaimer 2000). Radionuclides, especially the cosmogenic ones, have been widely used in astrophysics, in research on climate change, in environmental pollution studies, in dating of geological samples, and in dating of historical events and cultural heritage samples (e.g., Reimer et al. 2020; Usoskin et al. 2020; Mekhaldi et al. 2021; Povinec et al. 2021).

The closest source of cosmic radiation is the Sun (solar cosmic rays, SCR), emitting mainly protons during solar flare eruptions, which are accelerated in the solar corona and interplanetary space by shocks driven by coronal mass ejections to maximum energies of about 10 GeV. Such solar proton events (SPEs), also called solar energetic particle (SEPs) events (since they contain a few % of He and other nuclei), produce short but very intensive fluxes of energetic particles that could enter the Earth's atmosphere (Shea and Smart 2000; Usoskin 2013; Usoskin et al. 2020).

Galactic cosmic rays (GCR) are mostly composed of protons (87%) and α-particles (12%), with a smaller contribution (1%) from heavier nuclei, having proton energies between $1 - 10^{15}$ MeV (Dunai, 2010). After entering the heliosphere, they are significantly influenced by the Sun due to turbulent solar wind, accompanied by heliospheric magnetic fields. The GCR in the heliosphere, due to changes in the solar activity (mainly by the 11-year solar cycle), undergo large temporal variations in their intensity and energy. This modulation effect is important for proton energies between 0.020–20 GeV, having a maximum at 500 MeV, representing a variation in GCR flux by an order of magnitude over a solar cycle. The 11-year cycle in GCRs is delayed from a month up to two years with respect to the sunspot numbers which indicate the solar activity (Usoskin 2017).

As GCR and SCR are charged particles, they are affected by the Earth's magnetic field, which causes a shielding effect expressed by the cutoff rigidity[1] required for a particle to reach the Earth surface at a given location. Cosmic rays with higher rigidity are able to penetrate deeper into the atmosphere before being deflected or stopped by the Earth's magnetic field (especially at the poles, where the shielding effect of the geomagnetic field is weaker) (Masarik and Beer 1999, 2009).

Cosmic rays produce in the atmosphere cascades of secondary particles, including nucleons, which then participate in nuclear reactions with atmospheric atoms, producing cosmogenic radionuclides. After their formation, the radionuclides enter into atmosphere-hydrosphere-biosphere exchange processes, and finally they are deposited in isotope archives, carrying signals that were affecting their production and transport in the environment (e.g., Masarik and Beer 2009; Beer et al. 2012; Reimer et al. 2020; Shea and Smart 2000; Usoskin 2013; Usoskin et al. 2020; Mekhaldi et al. 2021).

[1]The particle rigidity is defined as R = pc/q, where p is the momentum of the particle, c is the speed of light in a vacuum and q is the charge of the particle.

https://doi.org/10.1017/RDC.2024.37 Published online by Cambridge University Press

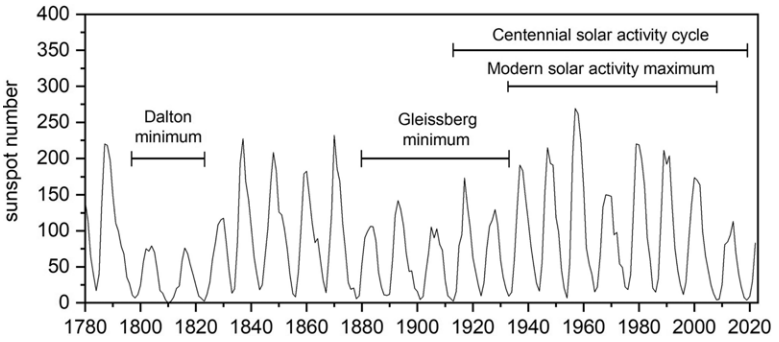

Figure 1 International sunspot numbers for the 19th and 20th century, indicating 11-year solar activity cycles, including Dalton (1797–1823) and Gleissberg (1878–1933) solar activity minima. The Centennial solar cycle (1913–2019) and the Modern solar activity maximum (1933–2008) can also be identified. Source: Royal Observatory of Belgium (https://www.sidc.be/SILSO/home).

In this paper, we review past radiocarbon variation studies in the biosphere (mainly tree rings), which were associated with changes in solar activity during 1785–1950, mostly represented by 11-year solar cycles (SCs), also called Schwabe cycles. As the Sun modulates the intensity of GCR in the heliosphere, it was reasonably expected that it could have an impact on the ^{14}C variations in the atmosphere and biosphere.

Stuiver (1961, 1965) was the first (using data of Willis et al. 1960) to notice an inverse correlation between ^{14}C levels in tree rings and Sun activity (sunspot numbers), suggesting a ^{14}C cycle with a period of ca. 100 yr (the Centennial solar cycle). The well-known Suess wiggles (Suess, 1980) had a characteristic period of ca. 200 yr (also called the Suess cycle). In both cases, the amplitude of the ^{14}C variations was estimated at 10–20‰.

The 11-Year Solar Cycles

The 11-year SCs have been recorded by regular observation of the number of sunspots on the Sun, well documenting the solar activity after AD 1700, although the first observations started in 1610. During the Maunder Grand solar minimum (1621–1718), almost no sunspots were observed, and later two weaker minima, the Dalton (1797–1823) and the Gleissberg (1878–1933), were identified (Figure 1) (Petrovay 2010; Gao 2016). The Centennial solar cycle (1913-2019) and the Modern solar activity maximum (1933-2008) can also be identified in the sunspot number record presented in Figure 1. It is interesting to note that during the Modern solar maximum the solar activity was higher than the sunspot number record (reconstructed from ^{14}C measurements in tree rings) over the last 8000 years (Solanki et al. 2004).

The solar activity has an impact on the flux of GCR in the heliosphere, which anti-correlates with 11-year SC and produces regular variations in the intensity of GCR in the Earth atmosphere. Although the 11-year SC is the most prominent cycle observed in solar activity, short-term ^{14}C variations are difficult to observe because of the complex mechanism of ^{14}C production by cosmic rays, its transport from the atmosphere to the ocean and biosphere, and climatic and reservoir influences. Lingenfelter and Ramaty (1970) did the first calculations of the ^{14}C production rates during the 11-year SC, which could vary from solar minimum to solar

https://doi.org/10.1017/RDC.2024.37 Published online by Cambridge University Press

maximum by 20–30%. Recently, more precise calculations by Usoskin et al. (2020) for the strongest 11-year SC (1954–1964, Figure 1) showed ^{14}C production rates ranging from 1.3 to 1.9 atoms cm^{-2} s^{-1}, (the varying factor of 1.5). However, because of the complicated carbon cycle, which acts as a buffer filtering the ^{14}C signal (Siegenthaler et al. 1980; Bard et al. 1997), the 11-year ^{14}C cycle is attenuated by a factor of ca. 100 to the magnitude of 1–3‰.

Damon et al. (1973a,b) performed the first high-precision ^{14}C measurements in annual tree-ring samples (1940–1954), which showed $\Delta^{14}C$ amplitude variation during the 11-year SC of around 2‰. These results were later confirmed in several other investigations (e.g., Povinec 1977, 1987; Burchuladze et al. 1980a, 1980b; Stuiver 1980, 1982; Stuiver and Quay 1980; Povinec et al. 1983; Attolini et al. 1989; Brehm et al. 2021).

Recently, another interesting phenomenon was investigated, when in addition to regular ^{14}C variations during the 11-year SCs, rapid ^{14}C increases up to 12‰ were found in tree rings, which could be associated with the emission of solar protons (e.g., Miyake et al. 2012, 2013; Usoskin, 2013; Usoskin et al. 2013, 2020; Mekhaldi et al. 2015, 2021; Park et al. 2017; Wang et al. 2017; Jull et al. 2018; O'Hare et al. 2019; Reimer et al. 2020; Brehm et al. 2021).

SAMPLES AND METHODS

Thanks to advanced radiometric methods for radiocarbon measurements, it has been possible to study even fine radiocarbon variations in the biosphere, which could be associated with the 11-year SC (Povinec 1977, 1987). A lime tree (*Tilia cordata*) from the Prešov region, Slovakia (48°52'N, 21°10'E) was used to develop the radiocarbon time series. The preparation of samples and ^{14}C counting using a low-background proportional counter was described by Povinec (1972, 1977, 1978). ^{14}C in Georgian wines (ca. 38°N, 45°E), obtained from the Tbilisi Museum of Wines, was analyzed using liquid scintillation decay counting (Burchuladze et al. 1980a, 1989). The typical standard deviations of the single measurements were 3‰ (at 1σ). Several cross-check measurements between the Bratislava and Tbilisi laboratories showed results that were indistinguishable within the statistical uncertainties.

The development of the AMS radiocarbon dating method has greatly benefited ^{14}C measurement in tree-ring studies thanks to decreasing the sample size below 1 mg of carbon and reducing the uncertainty of measurements down to 1.5‰ (e.g., Povinec et al. 2009; Miyake et al. 2012; Mekhaldi et al. 2015; Jull et al. 2018; Brehm et al. 2021).

Radiocarbon results are presented as $\Delta^{14}C$ values that are calculated relative to the ^{14}C oxalic acid standard of NIST (National Institute of Standards and Technology, Gaithersburg, USA), following the Stuiver and Polach (1977) approach.

RESULTS AND DISCUSSION

Radiocarbon Variations in Tree Rings and Wines (1902–1954)

We shall compare ^{14}C results obtained in tree-ring and wine samples collected in the first half of the 20th century that were measured by radiometric (Damon et al. 1973a, 1973b; Povinec 1977, 1987; Burchuladze et al. 1980a, 1980b; Stuiver 1980, 1982; Stuiver and Quay 1980; Attolini et al. 1989; Stuiver and Braziunas 1993) and AMS techniques (Brehm et al. 2021). As the GCRs are modulated by the Sun activity during the 11-year SC, it has been challenging to search for 11-year ^{14}C cycles in the biosphere. It was believed that the 11-year ^{14}C cycle would be difficult to observe, as short-term changes in radiocarbon production rates in the atmosphere will be too

https://doi.org/10.1017/RDC.2024.37 Published online by Cambridge University Press

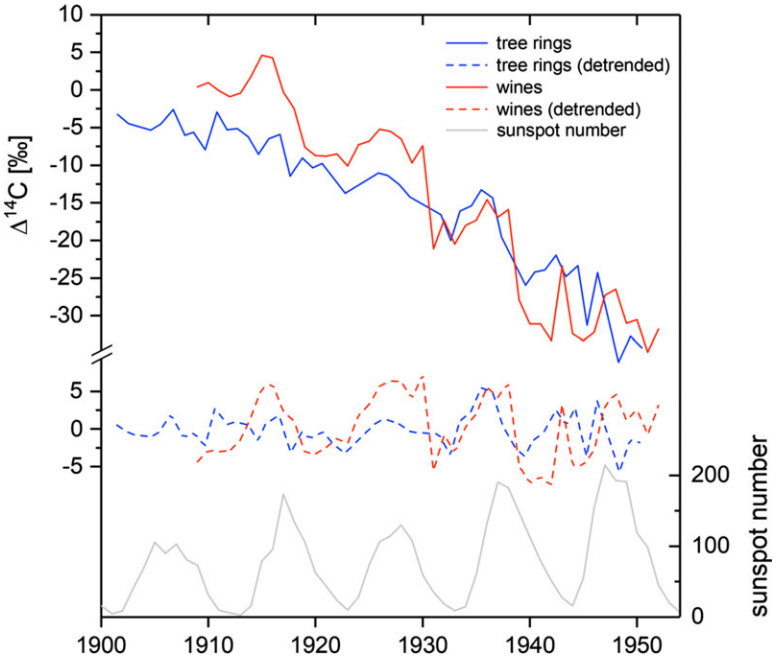

Figure 2 The $\Delta^{14}C$ record in tree rings (Povinec 1977, 1987) and wines (Burchuladze et al. 1980a) for the 20th century. The International sunspot number record is also shown (Royal Observatory of Belgium, http:/side-be/silso).

small to be observed in the biosphere due to a large reservoir buffer effect (Damon et al. 1973a, 1973b). However, radiocarbon measurements in tree rings and wines made in the 1970s showed that although the 11-year ^{14}C cycle is quite small, it is observable (Damon et al. 1973a, 1973b; Povinec 1977; Burchuladze et al. 1980a, 1980b; Stuiver 1980, 1982; Stuiver and Quay 1980). The $\Delta^{14}C$ levels in tree rings and wines corresponded well to the levels in the atmosphere at the time the tree rings (and grapes) were growing (Povinec et al. 1986; Burchuladze et al. 1989; Svetlik et al. 2010; Kontuľ et al. 2017, 2020). The radiometric ^{14}C results were later confirmed with AMS measurements carried out with much better precision (Brehm et al. 2021).

Unfortunately, after 1950, the natural 11-year ^{14}C cycle has been disrupted by anthropogenic ^{14}C produced during atmospheric nuclear weapons tests, which peaked in the biosphere in 1964 (ca. 100% above the natural level) (see, e.g., Burchuladze et al. 1989).

Another anthropogenic effect observed during the 19th and 20th century in the ^{14}C levels in the atmosphere and biosphere was due to growing amounts of CO_2 from fossil fuels that do not contain radiocarbon (Suess effect) (Suess 1955). Fortunately, as we shall discuss later, we can detrend the Suess effect from the annual $\Delta^{14}C$ data, and then compare the results with the sunspot number record.

Figure 2 shows radiocarbon variations in Bratislava tree rings (Povinec 1977, 1987) and Georgian wines (Burchuladze et al. 1980a) during five successive 11-year SCs for 1902–1954. We can clearly see a decreasing trend in $\Delta^{14}C$ levels due to the Suess effect, as well as the anticorrelation in radiocarbon variations with 11-year SCs (represented by sunspot numbers).

https://doi.org/10.1017/RDC.2024.37 Published online by Cambridge University Press

The non-statistical scatter of the results and the cyclic trend through the data indicate a possible dependence of $\Delta^{14}C$ data on the 11-year SC.

We applied several spectral analysis techniques to evaluate ^{14}C variations in tree-ring and wine samples. The spectral analysis of Bratislava tree-ring $\Delta^{14}C$ data for the 17th and 18th solar cycles showed an average 3‰ amplitude, an average 10-year periodicity and an average 3-year time lag, i.e., a delay in the $\Delta^{14}C$ record following the sunspot data (Table 1) (Povinec 1977; Burchuladze et al. 1980a). The delay between the $\Delta^{14}C$ maxima and the solar activity minima by ca. 3 years is caused by a time lag from the production of ^{14}C in the atmosphere to its uptake by the biosphere.

The Bratislava $\Delta^{14}C$ tree-ring data presented in Figure 2 were also analyzed using a cyclogram method, which is different from conventional power spectrum analysis with integrated harmonic components over time (Attolini et al. 1989). The cyclogram method enables one to follow the amplitude and phase variations with time for any component of a given periodicity. The $\Delta^{14}C$ phase and amplitude cyclograms were the most stretched for a period of 9 years, while the cross-cyclogram vectors showed the most regular behavior for a period of 10.5 years. The rms[2] $\Delta^{14}C$ amplitude computed through the cyclogram was 3‰ and the mean phase shift was 3 years (Table 1), confirming the anticorrelation dependence of $\Delta^{14}C$ on sunspot numbers (Attolini et al. 1989).

Harmonic analysis of Tbilisi wine samples for four 11-year SCs (1913–1954) of $\Delta^{14}C$ (t) data rows for wines and sunspot numbers (SN(t)) showed $\Delta^{14}C$ amplitudes of ca. 4‰ for different solar cycles (the average amplitude is 4.3 ± 0.2‰) with average periodicity of 11 years (Table 1). The time shift between the sunspot maxima and the delaying $\Delta^{14}C$ minima was 3–7 years (depending on the solar cycle), with an average value of 4 years. The correlation coefficients were between –0.6 and –0.9 (Burchuladze et al. 1980b). This anticorrelation between the decreasing solar activity and increasing ^{14}C production in the atmosphere is related to the modulation of GCR by the solar activity, as during the solar minimum there is an increased flux of GCR in the heliosphere and therefore also in the atmosphere of the Earth.

Furthermore, we applied spectral analysis, correlation analysis, and harmonic analysis to compare the $\Delta^{14}C$ results for wines (Burchuladze et al. 1980a) and tree-ring samples from the NW Pacific coast of USA (Stuiver and Braziunas 1993) using the same analysis technique. The results of the spectral analysis showed that for both types of samples, the autocorrelation functions had a quasi-periodic behavior with an 11-year period (at the 95% confidence interval). The autocorrelation functions had argument values $U_W = 10 \pm 1$ yr, $U_{trees} = 11 \pm 1$ yr, $U_{wines} = 11 \pm 1$ yr. The harmonic analysis showed the amplitude of $\Delta^{14}C$ variations in wines and tree rings for different solar cycles of 4.0–4.5‰ (±0.8‰) and 0.7–2.0‰ (±0.5‰), respectively. The average amplitude for wines and tree rings was 4.3 ± 0.2 and 1.5 ± 0.5‰, respectively. The average lag between SN(t) and $\Delta^{14}C$(t) rows for wines and tree rings was 4 and 2 years, respectively. The basic power of SN(t) and $\Delta^{14}C$(t) spectra was concentrated for a period of 11 years.

Recently Brehm et al. (2021) published a comprehensive data set of annual ^{14}C measurements in tree rings that covered the last millennium. We performed a harmonic analysis of the $\Delta^{14}C$ data for the period of 1902–1933 (tree rings from England) which showed the $\Delta^{14}C$ amplitudes from 0.8 to 1.8‰ (the average value of 1.2 ± 0.5‰), the average periodicity of 12 ± 1 years, and the average time lag of 3 years (Table 1).

[2]Root mean square (calculated by taking the square root of the mean of the squared values of the spectral amplitudes).

https://doi.org/10.1017/RDC.2024.37 Published online by Cambridge University Press

Table 1 Radiocarbon variation parameters for 11-year SCs in tree-ring and wine samples (1902–1954).

Samples	Time interval (yr)	$\Delta^{14}C$ amplitude (‰)					Average $\Delta^{14}C$ amplitude (‰)	Average periodicity (yr)	Average time shift (yr)
		14th SC 1902–1913	15th SC 1913–1923	16th SC 1923–1933	17th SC 1933–1944	18th SC 1944-1954			
Tree rings (US NW Pacific coast)[1]	1940–1954					2.1 ± 1.0	2.1 ± 1.0	10 ± 1	2 ± 1
Tree rings (Slovakia)[2]	1932–1952				2.8 ± 1.1	3.2 ± 1.2	3.0 ± 0.2	10 ± 1	3 ± 1
Tree rings (Slovakia)[3]	1902–1952	2 ± 1	2 ± 1	2 ± 1	3 ± 1	3 ± 2	3 ± 1	10 ± 1	3 ± 1
Tree rings (US NW Pacific coast)[4]	1916–1954	1.3 ± 0.5	2.0 ± 0.5	0.7 ± 0.4	2.0 ± 0.5		1.5 ± 0.5	11 ± 1	2 ± 1
Tree rings (England)[5]	1902–1933	0.8 ± 0.5	1.1 ± 0.5	1.8 ± 0.5			1.2 ± 0.5	12 ± 1	3 ± 1
Wines (Georgia)[6]	1909–1952		4.0 ± 0.8	4.3 ± 0.8	4.5 ± 0.9	4.3 ± 0.8	4.3 ± 0.2	11 ± 1	4 ± 1

References:
[1]Damon et al. 1973a
[2]Povinec 1977
[3]Attolini et al. 1989
[4]Stuiver and Braziunas 1993 (^{14}C data)
[5]Brehm et al. 2021 (^{14}C data)
[6]Burchuladze et al. 1980a

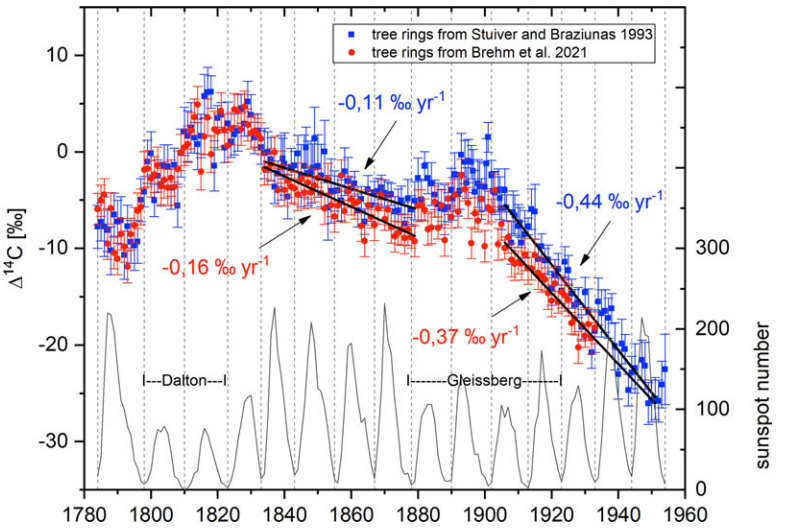

Figure 3 $\Delta^{14}C$ tree-ring results (with 2σ error bars) for the period of 1783–1954 obtained by Stuiver and Braziunas (1993) for the NW Pacific USA (gas counting) and for 1783–1933 obtained by Brehm et al. (2021) for England (AMS). The International sunspot number record is also shown (Royal Observatory of Belgium, http:/side-be/silso).

The results of the discussed radiocarbon studies during the five 11-year SCs for the period of 1902–1954 are presented in Table 1. We can see that a reasonable agreement within uncertainties has been obtained between samples of different origin (tree rings from Slovakia, England and NW Pacific coast, and wines from Georgia). The average $\Delta^{14}C$ amplitude derived from tree-ring samples is 2.2 ± 0.7‰, the average periodicity is 11 ± 1 years, and the average time lag between the sunspot numbers and $\Delta^{14}C$ records is 3 ± 1 years. Within uncertainties, these results are the same as those obtained for the wine samples.

Radiocarbon Variations in Tree-Ring Samples (1800–1950)

We performed a harmonic analysis of the $\Delta^{14}C$ tree-ring results for the period of 1783–1954 using the data of Stuiver and Braziunas (1993) and Brehm et al. (2021) obtained by gas counting and AMS, respectively. The purpose of the study was to compare the 11-year ^{14}C SCs measured in wood samples from the NW Pacific coast of the USA (Stuiver and Braziunas, 1993) and from England (Brehm et al. 2021). A comparison of $\Delta^{14}C$ tree-ring data presented in Figure 3 shows good agreement between both sets of data, although there are some differences. Generally, the Brehm et al. (2021) data after 1840 are ca. 5‰ lower than the Stuiver and Braziunas (1993) data, which could be due to the regional Suess effect. The NW Pacific is expected (also due to ocean influence) to be less affected by fossil fuel CO_2 contribution than the England location. It is interesting to note that the decline in ^{14}C levels for the years 1833–1880 and 1905–1952 had the same trend (–0.11‰ yr^{-1} and –0.44‰ yr^{-1} for the NW Pacific coast, and –0.16‰ yr^{-1} and –0.37‰ yr^{-1} for the western Europe (England), respectively), which is in reasonable agreement with modelling predictions of the Suess effect (Brehm et al. 2021).

The results of harmonic analysis of tree-ring samples covering twelve 11-year SCs (1798–1933) of $\Delta^{14}C$ data and sunspot numbers are presented in Table 2. The average $\Delta^{14}C$ amplitudes

https://doi.org/10.1017/RDC.2024.37 Published online by Cambridge University Press

Table 2 Radiocarbon variation parameters for 11-year solar cycles #5–16 in tree-ring samples (1798–1933).

	$\Delta^{14}C$ amplitude (‰)														
Origin of tree-ring samples	5th 1798–1810	6th 1810–1823	7th 1823–1833	8th 1833–1843	9th 1843–1855	10th 1855–1867	11th 1867–1878	12th 1878–1890	13th 1890–1902	14th 1902–1913	15th 1912–1923	16th 1923–1933	$\Delta^{14}C$[3] (‰)	P[4] (yr)	TS[5] (yr)
NW Pacific (USA)[1]	1.1 ± 0.5	1.2 ± 0.5	0.6 ± 0.4	0.4 ± 0.4	0.7 ± 0.5	1.8 ± 0.5	1.6 ± 0.5	1.7 ± 0.5	1.6 ± 0.5	1.3 ± 0.5	2.0 ± 0.5	0.7 ± 0.4	1.2 ± 0.5	10. 7 ± 2.1	4 ± 2
England[2]	1.8 ± 0.5	1.5 ± 0.5	0.7 ± 0.5	0.3 ± 0.3	0.4 ± 0.3	1.4 ± 0.5	1.0 ± 0.5	1.1 ± 0.5	1.6 ± 0.5	0.8 ± 0.5	1.1 ± 0.5	1.8 ± 0.5	1.1 ± 0.5	11.5 ± 1.7	5 ± 2

[1]Stuiver and Braziunas 1993
[2]Brehm et al. 2021
[3]Average $\Delta^{14}C$ amplitude
[4]Average periodicity
[5]Average time lag

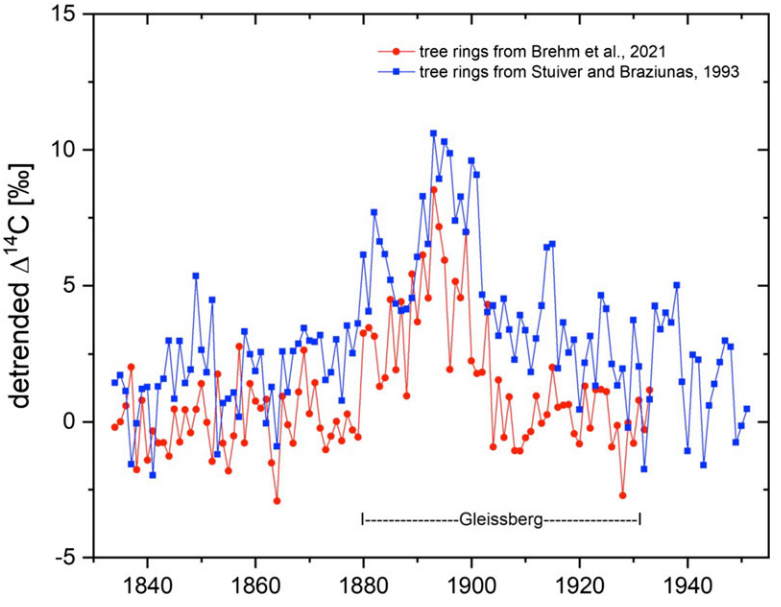

Figure 4 Detrended $\Delta^{14}C$ course for the period of 1835–1951 (extracted from Figure 3 after Suess effect corrections), confirming the existence of the Gleissberg minimum. To make trends and variations easier to see, error bars are not shown (see Figure 3). The International sunspot number record is also shown (Royal Observatory of Belgium, http:/side-be/silso).

derived from the data from Stuiver and Braziunas (1993) and Brehm et al. (2021) were very similar (1.2 ± 0.5‰ and 1.1 ± 0.5‰, respectively). The periodocities were in the range of 8–14 and 9–15 yr with mean values of 10.7 ± 2.1 and 11.5 ± 1.7 yr, respectively. The average time lags between the sunspot maxima and delaying $\Delta^{14}C$ minima were in the range of 1–7 and 2–9 yr with the average values of 4 ± 2 and 5 ± 2 yr), respectively. Therefore, the $\Delta^{14}C$ results obtained for the NW Pacific coast (measured by gas counting) and for England (measured by AMS) trees were the same within uncertainties.

Figure 3 also shows elevated $\Delta^{14}C$ levels during the Dalton minimum (1797–1823, covering two 11-year SCs with peak sunspot numbers around 75, Figure 1), which in the literature, similarly to the Maunder minimum, is also called Grand solar minimum (e.g., Brehm et al. 2021). Recently, several papers discussed parameters of the newly established Gleissberg minimum (1878–1933), with peak sunspot numbers in the range of 100–175 during cycle peaks, Figure 1 (e.g., Petrovay 2010; Komitov and Kaftan 2013; Gao 2016). Using the Gleissberg sunspot number filter (Gleissberg (1967), the length of this minimum was estimated to cover five 11-year SCs (Petrovay 2010; Gao 2016). Although this minimum was heavily affected by the Suess effect, especially after 1900, the $\Delta^{14}C$ data presented in Figure 3 clearly demonstrate its presence. For a better evaluation of its parameters, Figure 4 shows the detrended course of $\Delta^{14}C$ for the period of 1835–1951, after the corresponding corrections of the Suess effect. The detrended $\Delta^{14}C$ excess during the Gleissberg minimum in the Stuiver and Braziunas (1993) and Brehm et al. (2021) data is ca. 7‰ (similarly as in the case of the Dalton minimum). The duration of the minimum in $\Delta^{14}C$ data is, however, shorter: two 11-year SCs instead of five SCs (1878–1933) predicted by Petrovay (2010). This could be due to the fact that $\Delta^{14}C$ data

https://doi.org/10.1017/RDC.2024.37 Published online by Cambridge University Press

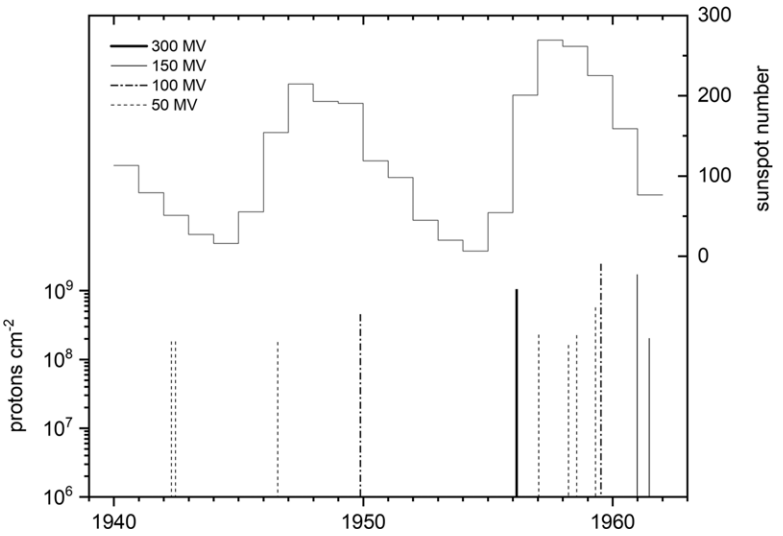

Figure 5 Total proton fluences during solar proton events with different proton rigidities, observed up to 1962. (Sources: Dorman and Mirosnicenko 1968; Shea and Smart 2020; Usoskin et al. 2020.)

covering the Gleissberg minimum were heavily affected by the Suess effect, therefore, more precise ^{14}C measurements would be required to improve its parameters.

In the case of the Dalton minimum, the $\Delta^{14}C$ data cover three SCs as predicted (Petrovay 2010). Actually, the normalized ^{14}C production rates calculated for the Dalton minimum by Brehm et al. (2021) may also suggest three SCs, although the generally accepted duration of the Dalton minimum covers only two cycles (1797–1823). Compared to the Maunder Grand solar minimum, the Dalton minimum could only be called a "semi-grand minimum", and the Gleissberg minimum should be an even weaker minimum (Petrovay 2010). Although it is longer in duration than the Dalton minimum, the number of sunspots is greater (> 100 in each SC). As the $\Delta^{14}C$ data presented in Figures 3 and 4 clearly demonstrate the existence of the Gleissberg minimum, we should take it into account when discussing impacts of solar activity on the biosphere.

Solar Proton Events

Solar proton events (SPEs), represented by emissions of energetic protons from the Sun, could influence the course of 11-year ^{14}C SCs in the atmosphere and biosphere (Lingenfelter and Ramaty 1970; Lingenfelter and Hudson 1980), since the anticorrelation between the ^{14}C variations and the solar activity could be affected, especially if total proton fluences are large ($>10^{10}$ p cm^{-2}), and their rigidity is also high (>100 MV) (Povinec 1975; Konstantinov et al. 1992).

In the 1970s we therefore searched for possible elevated $\Delta^{14}C$ levels in annual tree-ring data that could be associated with SPEs observed during the 1940s (Figure 5) (Povinec 1975, 1977). As the registered SPEs were too weak (both in proton fluencies and proton rigidities), the effects in ^{14}C production could be unobservable. However, these were the only registered SPEs that we could compare with our $\Delta^{14}C$ dataset.

https://doi.org/10.1017/RDC.2024.37 Published online by Cambridge University Press

The first interesting observation was that the large SPEs were usually observed before or after the maximum of the 11-year SC (Figure 5). This was also the case of the 23 February 1956 SPE that was observed close to the maximum of the 11-year SC. Unfortunately, as we already mentioned, natural ^{14}C levels during 1956 were already affected by global fallout from atmospheric nuclear bomb tests (Burchuladze et al. 1989), and therefore we could compare $\Delta^{14}C$ data only with SPEs that were observed in the first half of the 20th century.

The first documented solar bursts were observed by Forbush (1946) on February 28 and March 7, 1942. These SPEs were observed, however, two years before the solar minimum, i.e., at a time when the effects from these flares would be superimposed on the high GCR background observed during the 11-year SC. The second important point is that due to Forbush decreases (Forbush 1946), which represent rapid decreases in the GCR intensity following a coronal mass ejection when the magnetic field of the plasma solar wind sweeps the GCR away from the Earth, the ^{14}C production by the GCR should also decrease. Although it is expected that the SPEs of 1942 were much weaker than the 1956 SPE, it was interesting to search in the experimental $\Delta^{14}C$ data presented in Figure 2 for possible effects. We see in the tree-ring record two peaks with elevated $\Delta^{14}C$ values of 5‰ above the GCR background, which should be associated with the increased GCR background after the preceding solar activity minimum. Interestingly, the $\Delta^{14}C$ data of wine samples presented in Figure 2 show elevated $\Delta^{14}C$ values in 1943 (two measurements of –22.5 and –24.3‰, Burchuladze et al. 1980a). However, the expected decline of $\Delta^{14}C$ levels after this maximum is missing, therefore this peak cannot be associated with SPE. The Stuiver and Braziunas (1993) $\Delta^{14}C$ data (Figure 3 and 4) show a minimum value for 1943, and then rising values until 1947, i.e., this $\Delta^{14}C$ record cannot be associated with the SPE of 1942.

The second SPE was observed on 25 July 1946, which was a single event comparable to each of the two 1942 events, also accompanied by the Forbush decrease (Forbush, 1946). This flare originated before the solar maximum, and therefore its possible impact could be better observable because of a lower GCR background. The $\Delta^{14}C$ wine data show during 1947 and 1948 an elevation of 5‰ above the GCR background (Figure 2), however, the $\Delta^{14}C$ tree-ring data (Figure 2) and Stuiver and Braziunas (1993) data (Figure 3 and 4) do not show any increased values above the GCR background.

The SPE observed on 19 November 1949 (Adams and Braddick 1951) was the strongest (both in proton fluences and rigidities) when compared with the 1942 and 1946 events. The wine $\Delta^{14}C$ record (Figure 2) shows a minimum value for 1951 (0‰) and then an increase in 1952 (2.5‰), i.e., the data do not follow the expectations. It is likely that the increased $\Delta^{14}C$ value in 1952 was already influenced by the bomb effect, similarly as the Stuiver and Braziunas (1993) data (Figure 3). After 1955 (during the Modern solar activity maximum, Figure 1), many large solar proton flares occurred, however, because of the bomb effect, possible SPE impacts on ^{14}C production cannot be investigated (Burchuladze et al. 1989).

The origin of SPEs that originated before 1940 were not well documented. We should also mention that large solar superstorms producing large geomagnetic disturbances were not always accompanied by large SPEs. Although during the SPEs of 1942, 1946 and 1949 solar particles were registered together with radio disturbances, during some other solar super storms, such as the one observed in February 1958, the SPE was not registered. The special case is the Carrington event observed in September 1859, which was recognized as probably the biggest solar superstorm observed till now (Green and Boardsen 2006). However, the Brehm

https://doi.org/10.1017/RDC.2024.37 Published online by Cambridge University Press

et al. (2021) and Stuiver and Braziunas (1993) $\Delta^{14}C$ data (Figures 3 and 4) do not show any peak that could be associated with this event (actually, they show decreasing $\Delta^{14}C$ values after 1859).

Recent AMS analysis of annual tree rings revealed sharp increases in $\Delta^{14}C$ of 5–12‰ at AD 775 and 993 (Miyake et al. 2012, 2013). Usoskin et al. (2013), using more precise calculations of ^{14}C production rates, suggested the AD 775 event as possible consequence of a giant SPE. Furthermore, Usoskin et al. (2020) compared these SPEs with the one observed on 23 February 1956, which was the strongest directly observed SPE to date (10^9 p m^{-2}) with a very hard proton spectrum (rigidities >300 MV, Figure 5). The calculated $\Delta^{14}C$ signal from this SPE (due to attenuation of high-frequency signals by the carbon cycle) would be, however, only 0.2‰. As this value is comparable with the present uncertainty of ^{14}C analysis by AMS (1.5‰; Brehm et al. 2021), the effect of the SPE of 23 February 1956 (and similar SPEs) would be undetectable. The SPEs observed by Miyake et al. (2012, 2013), and also other events observed by other groups, and later confirmed by ^{10}Be and ^{36}Cl records in ice cores as well (Mekhaldi et al. 2015, 2021; Park et al. 2017; Wang et al. 2017; Jull et al. 2018; O'Hare et al. 2019; Brehm et al. 2021) should therefore be stronger than the 1956 SPE by about a factor of at least 25 (Usoskin et al. 2013, 2020).

Stuiver and Braziunas (1993) and Brehm et al. (2021) data (Figures 3 and 4) do not show clear peaks that could be associated with SPEs during 1800–1950. The disadvantage of ^{14}C for searching for SPEs is that small $\Delta^{14}C$ peaks would be difficult to observe in tree-ring samples because the carbon cycle damps high-frequency atmospheric signals by about a factor of 300 (Usoskin et al. 2020). The ^{10}Be signal, because of simpler atmospheric transport and its storage in ice, would have a better sensitivity than ^{14}C (although it is a product of high-energy spallation reactions). It is expected, however, that ^{36}Cl in ice cores could be an even better isotope tracer to identify SPEs, having advantages of ^{10}Be and ^{14}C (it is a low-energy product), and because high-sensitivity analysis of ^{36}Cl can be achieved with AMS (Mekhaldi et al. 2021).

The previous skepticism (which was common during the 1970s–1980s) about the possibility to observe short-term ^{14}C variations in tree rings has been dispelled, and many new well-defined $\Delta^{14}C$ increases have been investigated in tree-ring data covering the last millennia thanks to the availability of tree ring and ice core samples, and the high-precision AMS technique. As the $\Delta^{14}C$ levels in the atmosphere are currently close to zero due to decline in the bomb effect (Kontul' et al. 2022; Povinec et al. 2024a, 2024b), this opens a new window to study recent impacts of SPEs on ^{14}C production in the atmosphere and biosphere using much better datasets on the characteristics of SPEs, mostly obtained from satellites.

The SPEs have been of major concern to society with regard to possible negative impacts on electronic infrastructure as well as for long-term space missions. Therefore, better understanding of the frequency of their occurrence in past millennia, as well as of the emitted proton fluxes, will help in prediction and preparation for their future impacts.

CONCLUSIONS

Cosmogenic radiocarbon has proved to be an important tracer for studying solar activity impacts on the biosphere, including 11-year solar activity cycles, as well as impacts of solar protons on ^{14}C production in the atmosphere and its transport to the biosphere. Observations of thirteen 11-year ^{14}C solar activity cycles (1798–1944) in annual tree-ring samples from the NW Pacific coast of USA (Stuiver and Braziunas 1993) and from England (Brehm et al. 2021)

https://doi.org/10.1017/RDC.2024.37 Published online by Cambridge University Press

discussed in this review showed the average $\Delta^{14}C$ amplitude of 1.3 ± 0.3‰, the average periodicity of 11 ± 1 yr, and the average time lag between the sunspot numbers and $\Delta^{14}C$ records of 3 ± 1 yr. The $\Delta^{14}C$ data after 1840 for England were ca. 5‰ lower than the data for the NW Pacific coast, which could be due to the regional Suess effect. The decline in ^{14}C levels for the years 1833–1880 and 1905–1953 had the same trend at the two sites (–0.11‰/year and –0.44‰/year for the NW Pacific, and –0.16‰/year and –0.37‰/year for Europe, respectively).

The $\Delta^{14}C$ tree-ring data discussed for the NW Pacific (USA) and England clearly demonstrated the presence of the Dalton minimum (1797–1823), as well as the existence of the new Gleissberg minimum (1878–1933). The observed $\Delta^{14}C$ excess during the Dalton and Gleissberg minima was ca 7‰. Although the Gleissberg minimum was heavily affected by the Suess effect (especially after 1900), the $\Delta^{14}C$ data (for the first time) clearly demonstrate its existence, and therefore the Gleissberg minimum should be taken into account when discussing impacts of solar activity on the biosphere.

The discussed $\Delta^{14}C$ tree-ring data for the period of 1800–1950 did not show any elevated levels above the GCR background, which could be associated with solar proton events, because they were ca. at least an order of magnitude smaller than the giant events producing sharp increases in annual tree-ring $\Delta^{14}C$ data during the first millennium AD (Miyake et al. 2012, 2013; Brehm et al. 2021). There have been many discussions about the ^{14}C records associated in the past with giant SPEs, also accompanied with ^{10}Be and ^{36}Cl records in ice cores, which have been of great concern to society with regard to possible negative impacts on electronic infrastructure, as well as for long-term space missions.

Investigations carried out during the last 50 years confirmed that solar phenomena (solar activity cycles and solar proton events) are an important and practical part of radiocarbon research aimed at better understanding the Sun's behavior and its impact on the Earth's environment.

ACKNOWLEDGEMENTS

A support under the Operational Program Integrated Infrastructure for the project "Advancing University Capacity and Competence in Research, Development and Innovation (ACCORD)", (ITMS2014+:313021X329, co-financed by the European Regional Development Fund), and the support from the Slovak Research and Development Agency (projects APV-15-0576 and APVV-21-0377), and the Slovak Science and Grant Agency (project VEGA-1/0625/21) is highly acknowledged.

REFERENCES

Adams N, Braddick HJ. 1951. Time and other variations in the intensity of cosmic ray neutrons. Z. Naturforsch 6a:592–598.

Attolini MR, Galli M, Nanni T, Povinec P. 1989. A cyclogram analysis of the Bratislava ^{14}C tree-ring record during the last century. Radiocarbon 31:839–845.

Bard E, Raisbeck G, Yiou F, Jouzel J. 1997. Solar modulation of cosmogenic nuclide production over the last millennium: comparison between ^{14}C and ^{10}Be records. Earth Planet. Sci. Lett. 150: 453–462. doi: 10.1016/S0012-821X(97)00082-4

Beer J, McCracken K, von Steiger R. 2012. Cosmogenic radionuclides: theory and applications in the terrestrial and space environments. Berlin: Springer.

Brehm N, Bayliss A, Christl M, Synal HA, Adolphi F, Beer J, Kromer B, Muscheler R, Solanki SK, Usoskin I, Bleicher N, Bollhalder S, Tyers C, Wacker L. 2021. Eleven-year solar cycles over the last millennium revealed by radiocarbon in tree rings. Nature Geoscience 14:10–15. www.nature.com/naturegeoscience.

Burchuladze AA, Chudý M, Eristavy IV, Pagava SV, Povinec P, Šivo A, Togonidze GI. 1989.

https://doi.org/10.1017/RDC.2024.37 Published online by Cambridge University Press

Anthropogenic ^{14}C variations in atmospheric CO_2 and wines. Radiocarbon 31:771–776.
Burchuladze AA, Pagava SV, Povinec P, Togonidze GI, Usačev S. 1980a. Radiocarbon variations with the 11-yr solar cycle during the last century. Nature 287:320–322.
Burchuladze AA, Pagava SV, Povinec P, Usačev S. 1980b. Radiocarbon and investigation of 11-y variations of cosmic rays in the past. Reports of USSR Academy of Science 44:2347–2351.
Damon PE, Long A, Grey DC. 1970. Arizona radiocarbon dates for dendrochronologically dated samples. In: Olsson IU, editor. Radiocarbon variations and absolute chronology, Nobel symposium 12, Internatl. radiocarbon conf, 7th, Proc: Stockholm, Almqvist & Wiksell. p. 615–618.
Damon PE, Long A, Wallick EI. 1973a. On the magnitude of the 11-year radiocarbon cycle. Earth Planet. Sci. Lett. 20:300–306.
Damon PE, Long A, Wallick EI. 1973b. Comments on "Radiocarbon: Short-term variations" by M.S Baxter and J.G. Farmer. Earth Planet. Sci. Lett. 20:307–310.
Dorman LI, Mirosnicenko LI. 1968. Solar cosmic rays. Moscow: Nauka.
Dunai TJ. 2010. Cosmogenic nuclides. London: Cambridge University Press. doi: 10.1017/CBO9780511804519
Forbush SE. 1946. Three unusual cosmic-ray increases possibly due to charged particles from the Sun. Physical Review 70:771–772.
Gao PX. 2016. Long-term trend of sunspot numbers. Astrophys. J. 830:140. doi: 10.3847/0004-637X/830/2/140
Gleissberg W. 1967. Secularly smoothed data on the minima and maxima of sunspot frequency. Solar Phys. 2: 231–233.
Green JL, Boardsen S. 2006. Duration and extent of the great auroral storm of 1859. Adv. Space Res. 38:130–135.
Jull AJT, Panyushkina I, Miyake F, Masuda K, Nakamura T, Mitsutani T, Lange TE, Cruz RJ, Baisan C, Janovics R, Varga T, Molnár M. 2018. More rapid ^{14}C excursions in the tree-ring record: a record of different kind of solar activity at about 800 BC? Radiocarbon 60:1237–1248.
Komitov B, Kaftan V. 2013. The sunspot cycle no. 24 in relation to long term solar activity variation. J. Adv. Res. 4:279–282. doi: 10.1016/j.jare.2013.02.001
Konstantinov AN, Levchenko VA, Kocharov GE, Mikheva IB, Chechini S, Galli M, Nani T, Povinec P, Rugiero L, Salomoni A. 1992. Theoretical and experimental aspects of solar flares manifestation in radiocarbon abundances in tree rings. Radiocarbon 34:247–253.
Kontuľ I, Ješkovský M, Kaizer J, Šivo A, Richtáriková M, Povinec PP, Čech P, Steier P, Golser R. 2017. Radiocarbon concentration in tree-ring samples collected in the south-west Slovakia (1974–2013). Applied Radiation and Isotopes 126:58–60.
Kontuľ I, Povinec PP, Richtáriková M, Svetlik I, Šivo A. 2022. Tree rings as archives of atmospheric pollution by fossil carbon dioxide in Bratislava. Radiocarbon 64:1577–1585.
Kontuľ I, Svetlik I, Povinec PP, Brabcová KP, Molnár M. 2020. Radiocarbon in tree rings from a clean air region in Slovakia. Journal of Environmental Radioactivity 218:106237.
Lal D. 1999. An overview of five decades of studies of cosmic ray produced nuclides in oceans. The Science of the Total Environment 237/238:3–13.
Lal D, Peters B. 1967. Cosmic ray produced radioactivity on the Earth. In: Sittle K, editor. Handbuch der Physik 9/46/2:551–612. Berlin: Springer. doi: 10.1007/978-3-642-46079-1_7.
Levin I, Hesshaimer V. 2000. Radiocarbon – a unique tracer of global carbon cycle dynamics. Radiocarbon 42:69–80. doi: 10.1017/S0033822200053066
Lingenfelter RE, Hudson HS. 1980 Solar particle fluxes and the ancient Sun. In: Pepin RO, Eddy JA, Merrill RB, editors. The Ancient Sun. New York: Pergamon Press. p. 69–75.
Lingenfelter RE, Ramaty R. 1970. Astrophysical and geophysical variations in C-14 production. In: Olsson IU, editor. Radiocarbon variations and absolute chronology. Stockholm: Almqvist & Wiksell. p. 513–535.
Masarik J, Beer J. 1999. Simulation of particle fluxes and cosmogenic nuclide production in the Earth's atmosphere. Journal of Geophysical Research 104:12,099–12,111.
Masarik J, Beer J. 2009. An updated simulation of particle fluxes and cosmogenic nuclide production in the Earth's atmosphere. Journal of Geophysical Research 114:D11103. doi: 10.1029/2008JD010557
Mekhaldi F, Adolphi F, Herbs F, Muscheler R. 2021. The signal of solar storms embedded in cosmogenic radionuclides. Detectability and uncertainties. Journal of Geophysical Research: Space Physics 126:e2021JA029351.
Mekhaldi F, Muscheler R, Adolphi A, Aldahan A, Beer J, McConnell JR, Possnert G, Sigl M, Svensson A, Synal HA, Welten KC, Woodruff TW. 2015. Multiradionuclide evidence for the solar origin of the cosmic-ray events of AD 774/5 and 993/4. Nature Communications 6:8611.
Miyake F, Masuda K, Nakamura T. 2013. Another rapid event in the carbon-14 content of tree rings. Nature Communications 4:1748.
Miyake F, Nagaya K, Masuda K, Nakamura T. 2012. A signature of cosmic-ray increase in AD 774-775 from tree rings in Japan. Nature 486: 240–242. https://doi.org/10.1038/nature11123
O'Hare P, Mekhaldi F, Adolphi F, Raisbeck G, Aldahan A, Anderberg E, et al. 2019. Multiradionuclide evidence for an extreme solar proton event around 2,610 B.P. (660 BC).

https://doi.org/10.1017/RDC.2024.37 Published online by Cambridge University Press

Proceedings of the National Academy of Sciences 116(13):5961–5966.
Park J, Southon J, Fahrni S, Creasman PP, Mewaldt R. 2017. Relationship between solar acitvity and $\Delta^{14}C$ in AD 775, AD 994, and 660 BC. Radiocarbon 59:1147–1156.
Petrovay K. 2010. Solar cycle prediction. Living Rev. Sol. Phys. 7:6. doi: 10.12942/lrsp-2010-6
Povinec P. 1972. Preparation of methane gas for proportional ^{3}H and ^{14}C counters. Radiochem. Radioanal. Letters 9:127–135.
Povinec P. 1975. Production of isotopes in the Earth atmosphere by solar flare particles. In: Proc. Leningrad Symp. 263–275. IPI, Leningrad.
Povinec P. 1977. Influence of the 11-year solar cycle on the radiocarbon variations in the atmosphere: Acta Phys. Univ. Comen. 18:139–149.
Povinec P. 1978. Multiwire proportional counters for low-level ^{14}C and ^{3}H counting. Nucl. Instr. Methods 156:441–446.
Povinec P. 1987. History of cosmic rays by cosmogenic radionuclides. Proc. 20th Intern. Cosmic-ray Conf. 7:115–137. IUPAP, Moscow.
Povinec P, Burchuladze AA, Pagava SV. 1983. Short term variations in radiocarbon concentration with the 11-year solar cycle. Radiocarbon 25: 259–266.
Povinec P, Chudý M, Šivo A. 1986. Anthropogenic radiocarbon: past, present and future. Radiocarbon 28:668–672.
Povinec PP, Hirose K, Aoyama M. 2013. Fukushima accident. Radioactivity impact on the environment. New York: Elsevier. 385 p.
Povinec PP, Hirose K, Aoyama M, Tateda Y. 2021. Fukushima accident: 10 years after. New York: Elsevier. 560 p.
Povinec PP, Kontuľ I, Ješkovský M, Kaizer J, Richtáriková M, Šivo A, Zeman J. 2024a. Long-term radiocarbon variation studies in the air and tree rings of Slovakia. J. Environ. Radioact. 274: 107401.
Povinec PP, Kontuľ I, Ješkovský M, Kaizer J, Kvasniak J, Pánik J, Zeman J. 2024b. Development of accelerator mass spectrometry methods for measurement of ^{14}C, ^{10}Be and ^{26}Al in the CENTA laboratory. J. Radioanal. Nucl. Chem. https://doi.org/10.1007/s10967-023-09294-5
Povinec PP, Litherland AE, von Reden KF. 2009. Developments in radiocarbon technologies: From the Libby counter to compound-specific AMS analyses. Radiocarbon 51:45–78.
Reimer PJ et al. 2020. IntCal20 Northern Hemisphere radiocarbon age calibration curve (0–55 cal kBP) and Marine13 radiocarbon age calibration curves 0–50,000 years cal BP. Radiocarbon 62: 725–757.
Shea MA, Smart DF. 2000. Fifty years of cosmic radiation data. Space Sci. Rev. 93:229–262.
Siegenthaler U, Heimann M, Oeschger H. 1980. ^{14}C variations caused by changes in the global carbon cycle. Radiocarbon 22:177–191.
Solanki SK, Usoskin IG, Kromer B, Schüssler M, Beer J. 2004. Unusual activity of the Sun during recent decades compared to the previous 11,000 years. Nature 431:1084–1087.
Stuiver M. 1961. Variations in radiocarbon concentration and sunspot activity. J. Geophys. Res. 66:273–276.
Stuiver M. 1965. Carbon-14 content of 18th- and 19th-century wood: variations correlated with sunspot activity. Science 149:533–535.
Stuiver M. 1980. Solar variability and climatic-change during the current millennium. Nature 286:868–871.
Stuiver M. 1982. A high precision calibration of the AD radiocarbon time scale. Radiocarbon 24:1–26.
Stuiver M, Braziunas TF. 1993. Sun, ocean, climate and atmospheric $^{14}CO_2$: an evaluation of causal and spectral relationships. Holocene 3:289–30.
Stuiver M, Polach HA. 1977. Discussion: reporting of ^{14}C data. Radiocarbon 19:355–363.
Stuiver M, Quay, PD. 1980. Changes in atmospheric carbon-14 attributed to a variable sun. Science 207:1–19.
Suess H. 1980. The radiocarbon record in tree rings of the last 8000 years. Radiocarbon 22:200–209.
Suess HE. 1955. Radiocarbon concentration in modern wood. Science 122:415–417.
Svetlik I, Povinec PP, Molnár M, Vána M, Sivo A, Bujtás T. 2010. Radiocarbon in the air of Central Europe: long-term investigations. Radiocarbon 52:823–834.
Usoskin G. 2013. A history of solar activity over millennia. Living Rev. Solar Phys. 10:1. http://www.livingreviews.org/lrsp-2013-1 doi: 10.12942/lrsp-2013-1
Usoskin G. 2017. A history of solar activity over millennia. Living Rev. Solar Phys. 14:3. doi: 10.1007/s41116-017-0006-9
Usoskin G, Kromer B, Ludlow F, Beer J, Friedrich M, Kovaltsov GA, Solanki SK, Wacker L. 2013. The AD775 cosmic event revisited: the Sun is to blame. Astron. Astrophys. 552:L3.
Usoskin IG, Koldobskiy SA, Kovaltsov GA, Rozanov EV, Sukhodolov TV, Mishev AL, Mironova IA. 2020. Revisited reference solar proton event of 23 February 1956: assessment of the cosmogenic-isotope method sensitivity to extreme solar events. J. Geophys. Res. Space Phys. 125:e2020JA027921.
Wang FY, Yu H, Zou YC, Dai ZG, Cheng KS. 2017. A rapid cosmic-ray increase in BC 3372–3371 from ancient buried tree rings in China. Nature Communications 8:1487.
Willis E, Tauber H, Münnich K. 1960. Variations in the atmospheric radiocarbon concentration over the past 1300 years. Radiocarbon 2:1–4.

https://doi.org/10.1017/RDC.2024.37 Published online by Cambridge University Press